Available online at www.sciencedirect.com

SciVerse ScienceDirect

Ceramics International 38 (2012) 5293–5297

CERAMICS INTERNATIONAL

www.elsevier.com/locate/ceramint

Short communication

Effect of pressure loading cycle on spark plasma sintered ZrB_2–SiC–Yb_2O_3 ceramics

Wei-Ming Guo [a,c], Zhen-Guo Yang [a,*], Jef Vleugels [b,*], Guo-Jun Zhang [c,*]

[a] Department of Materials Science, Fudan University, Shanghai 200433, China

[b] Department of Metallurgy and Materials Engineering, Katholieke Universiteit Leuven, Kasteelpark Arenberg 44, B-3001 Leuven, Belgium

[c] State Key Laboratory of High Performance Ceramics and Superfine Microstructures, Shanghai Institute of Ceramics, Shanghai 200050, China

Received 20 February 2012; received in revised form 22 February 2012; accepted 23 February 2012
Available online 3 March 2012

Abstract

The influence of the pressure loading cycle on spark plasma sintered ZrB_2–SiC–Yb_2O_3 ceramics was investigated. Spark plasma sintering consists of three stages, i.e., a heating-up, isothermal and cooling stage. Applying the load during isothermal stage allowed evaporation of volatile species. Applying the load during the heating-up and isothermal stages resulted in the entrapment of volatile species and the formation of nanometer-sized spherical SiO_2 particles. The presence of SiO_2 particles led to a large thermal residual stress, and improved fracture toughness in the ZrB_2–SiC–Yb_2O_3 ceramics.

Keywords: ZrB_2–SiC–Yb_2O_3; Spark plasma sintering; Pressure loading cycle; Microstructure; Fracture toughness

1. Introduction

ZrB_2-based ceramics are especially promising for high-temperature structural applications, such as cutting tools, thermal protection for hypersonic vehicles, molten metal crucibles, etc. owing to their unique properties such as high melting temperature, high strength, high thermal and electrical conductivity, and excellent resistance to thermal shock and oxidation [1,2]. ZrB_2-based ceramics have typically been densified by hot pressing (HP) at high temperature with a 1–2 h holding time, which in turn leads to grain growth and thus limited strength. In comparison with conventional HP, spark plasma sintering (SPS) allows to densify ZrB_2-based ceramics within minutes applying a very fast heating and cooling rate cycle [2–10].

To further adjust the microstructure and improve the mechanical properties of SPSed ZrB_2-based ceramics, the effect of various sintering parameters including temperature, holding time, heating rate, and pressure were conducted. Guo et al. systematically studied the effect of heating rate, soaking time, and sintering temperature on the microstructure of SPS ZrB_2 ceramics, revealing that a rapid grain growth was observed at high sintering temperature, slow heating rates, and long holding times [6]. The density of SPS ZrB_2–SiC composites was reported to increase with increased holding time and pressure, and prolonging the holding time could improve the fracture toughness [8]. We recently reported on the influence of the heating rate on densification, microstructure, and strength of SPS ZrB_2–SiC composites with or without Yb_2O_3 addition, showing that a low heating rate induced grain growth and slightly increased the strength of the Yb_2O_3-free ceramics, whereas the grain size was hardly influenced and the strength decreased in Yb_2O_3 doped composites [9].

Typically, spark plasma sintering comprises three stages, i.e. a fast heating-up stage, a short isothermal dwell stage, and a rapid cooling stage. The mechanical pressure can be applied at any moment during the thermal cycle. The influence of the pressure loading cycle on the microstructure and fracture toughness of SPS ZrB_2–SiC–Yb_2O_3 is investigated.

2. Experimental procedure

The raw materials used were ZrB_2 (Grade B, 2 μm, H.C. Starck, Karlsruhe, Germany), SiC (Grade HSC-059, 0.7 μm,

* Corresponding authors.
E-mail addresses: guo1238@126.com (W.-M. Guo), zgyang@fudan.edu.cn (Z.-G. Yang), jozef.vleugels@mtm.kuleuven.be (J. Vleugels), gjzhang@mail.sic.ac.cn (G.-J. Zhang).

0272-8842/$36.00
doi:10.1016/j.ceramint.2012.02.072

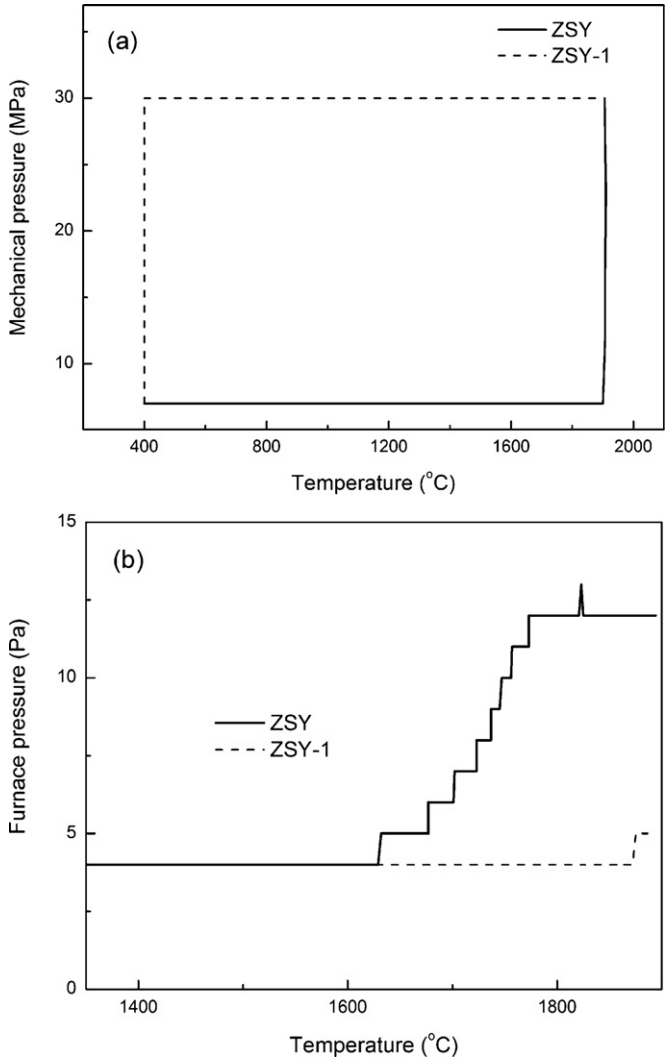

Fig. 1. Mechanical load (a) and vacuum evolution (b) in the furnace as a function of temperature during the SPS process.

Superior Graphite, USA), Yb_2O_3 (99.9%, ChemPur, Germany), and analytical grade nitric acid (65%). The starting powder composition of the investigated ZrB_2–SiC–Yb_2O_3 ceramics contained 75 vol% ZrB_2, 20 vol%SiC and 5 vol% Yb_2O_3. A colloidal suspension coating technique was used to incorporate the Yb_2O_3. The same coating technique was successfully applied to produce rare earth oxide doped ZrO_2 powders for the synthesis of tetragonal zirconia polycrystalline ceramics [11]. First, the appropriate amount of Yb_2O_3 was dissolved in nitric acid to obtain a clear nitrate solution. Subsequently, the solution was mixed with ZrB_2 and SiC powders in a polyethylene jar using ethanol and ZrO_2 milling balls (grade TZ-3Y, Tosoh, Tokyo, Japan) for 24 h, followed by rotating evaporation to remove the solvent. After drying, the powder mixture was put into a graphite die/punch set-up lined with graphite paper and densified by SPS (Type HP D 25/1, FCT Systeme, Rauenstein, Germany). Details on the experimental SPS set-up are provided elsewhere [12]. SPS was performed at 1900 °C for 4 min in vacuum with a heating rate of 100 °C/min. Fig. 1(a) shows the mechanical load during the SPS process. In the ZSY ceramics, the initial mechanical load of 7 MPa was increased to 30 MPa within 1 min upon reaching 1900 °C. In the ZSY-1 ceramics, the pressure was already increased from 7 to 30 MPa within 1 min at 400 °C. The pressure was released at the onset of cooling.

The microstructure was observed by scanning electron microscopy (SEM, XL-30FEG, FEI, Eindhoven, The Netherlands) equipped with backscattered electron imaging (BSE), and transmission electron microscopy (TEM, JEM2100, JEOL, Japan). The fracture toughness was measured by the Vickers indentation method (Model FV-700, Future-Tech Corp., Tokyo, Japan) using a load of 98 N for 10 s on a polished surface.

3. Results and discussion

Backscattered electron images of polished surfaces of ZSY and ZSY-1 are shown in Fig. 2. The ZSY ceramics contain a grey ZrB_2 matrix with a dispersed dark SiC phase and an additional white contrast phase, as shown in Fig. 2(a). We have previously reported the XRD results of ZSY ceramics [9,10]. Based on XRD analysis, the white phase was identified as $Yb_2Zr_8O_{19}$ (ICDD 78-1309) and $YbBO_3$ (ICDD 19-1427), formed by the reaction of ZrO_2 and B_2O_3 with Yb_2O_3 [9,10]. Because of the small difference in mean atomic number, the $Yb_2Zr_8O_{19}$ and $YbBO_3$ phases cannot be differentiated by BSE contrast. Although the XRD patterns of the ZSY-1 and ZSY

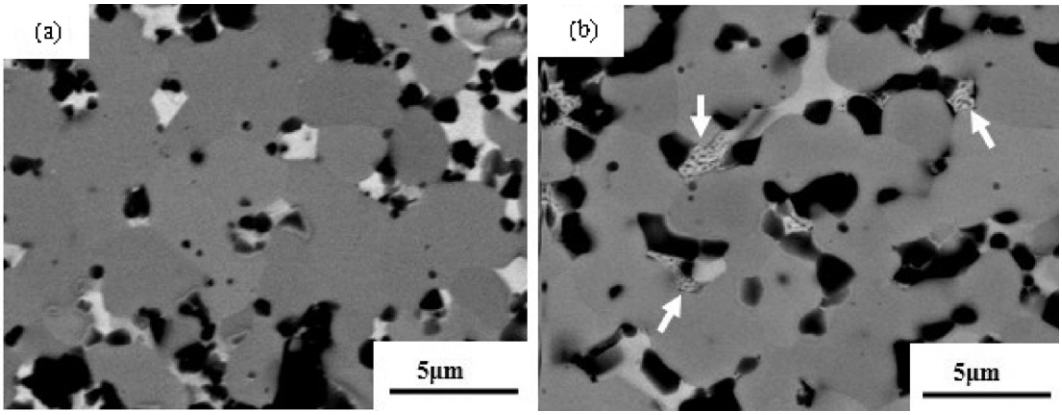

Fig. 2. Backscattered electron images of polished surfaces of ZSY (a) and ZSY-1 (b).

ceramics completely coincided, an additional white phase with darker dispersed features is present in the microstructure of ZSY-1, as indicated by the white arrows in Fig. 2(b). Transmission electron microscopy (TEM) images of the grain boundary composite structure are shown in Fig. 3. The TEM image in combination with EDX point analysis revealed that the black spots were 100–200 nm sized spherical SiO_2 particles. The SiO_2 particles were mostly present in the multiple grain junctions.

It is well-known that SiO_2 and B_2O_3 are present on the surface of SiC and ZrB_2 powders, respectively. During thermal treatment, the B_2O_3 and SiO_2 dissolve forming borosilicate glass (SiO_2–B_2O_3) in ZrB_2–SiC ceramics [13]. XRD analysis of ZrB_2–SiC–Yb_2O_3 ceramics revealed that the Yb_2O_3 can react with B_2O_3 from the borosilicate glass to form $YbBO_3$ [9–10]. Due to the consumption of B_2O_3, the borosilicate glass changed into SiO_2. Under vacuum and high temperature conditions, SiO_2 can be reduced by SiC as follows [14]:

$$2SiO_2 + SiC \rightarrow 3SiO\,(g) + CO\,(g) \quad (1)$$

In an open porous ceramic system, such as during heating under low load conditions like for ZSY, SiO vapour could readily be removed under the applied vacuum conditions, which would even further promote reaction (1) to proceed to completion. This would explain the fact that SiO_2 particles were not observed in the ZSY ceramics. When the pressure, however, was pre-applied during the heating-up stage, the escape of gaseous SiO was limited or even inhibited resulting in the precipitation of SiO_2 in the ZSY-1 ceramics. The evaporation of volatile species during SPS of ZSY and the absence of that during SPS of ZSY-1 are proven by the vacuum level evolution in the furnace as a function of temperature, as shown in Fig. 1(b). The furnace pressure during SPS of ZSY clearly increased above about 1600 °C, whereas the vacuum level remained constant during SPS of ZSY-1.

The fracture toughness of ZSY-1, 4.3 ± 0.1 MPa $m^{1/2}$, was approximately 21% higher than for ZSY, 3.5 ± 0.1 MPa $m^{1/2}$. To elucidate the toughening mechanisms induced by changing the pressure loading cycle, fracture surfaces of ZSY and ZSY-1 were investigated by SEM, as shown in Fig. 4. The microstructure of both ceramic grades consisted of equiaxed ZrB_2 and SiC grains and the fracture surfaces revealed a transgranular fracture. Although the coefficient of thermal expansion (CTE) of $Yb_2Zr_8O_{19}$ and $YbBO_3$ phases are not known, the CTE of ZrB_2 (6.5×10^{-6} °C^{-1}) and SiC (4.7×10^{-6} °C^{-1}) are substantially higher than for SiO_2 (0.5×10^{-6} °C^{-1}). Due to the large thermal expansion mismatch, very rapid cooling during SPS could introduce a

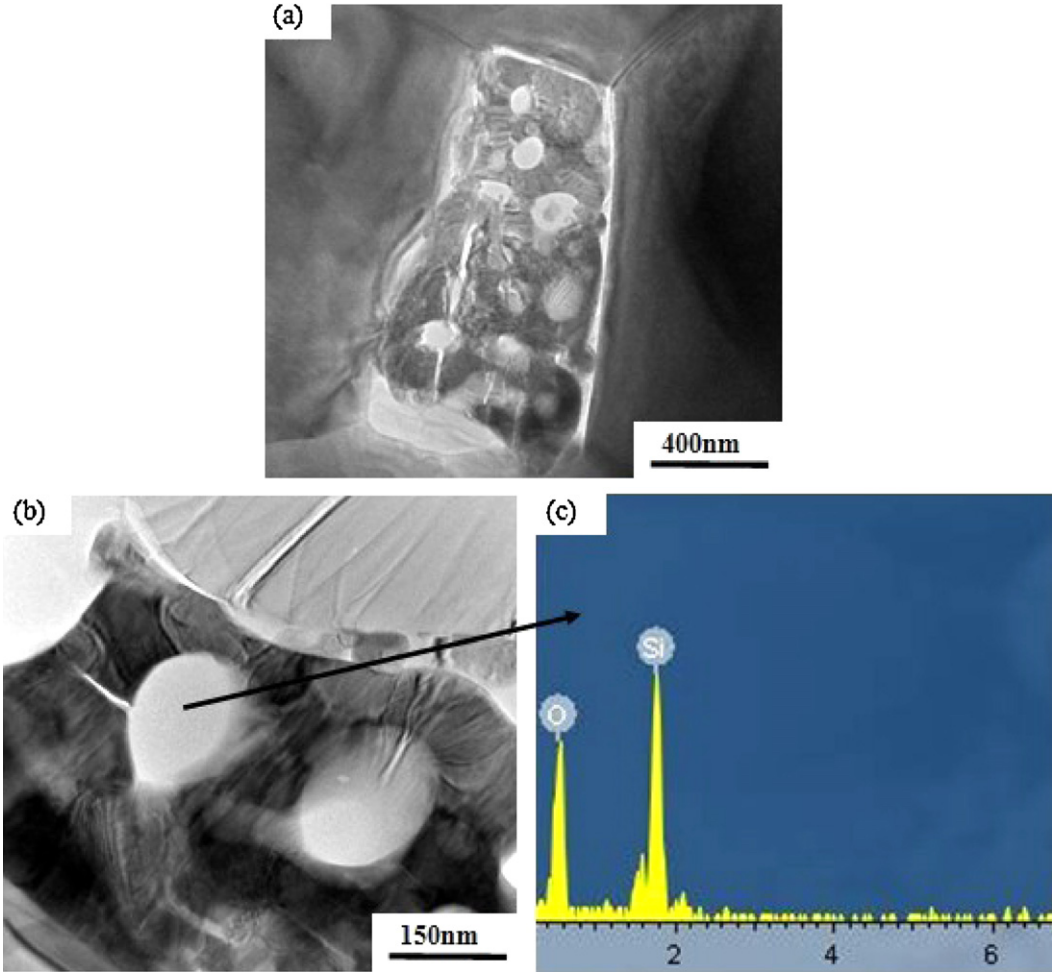

Fig. 3. Low (a) and high (b) magnification TEM images and EDS point analysis (c) of the spherical phase in the ZSY-1 ceramics.

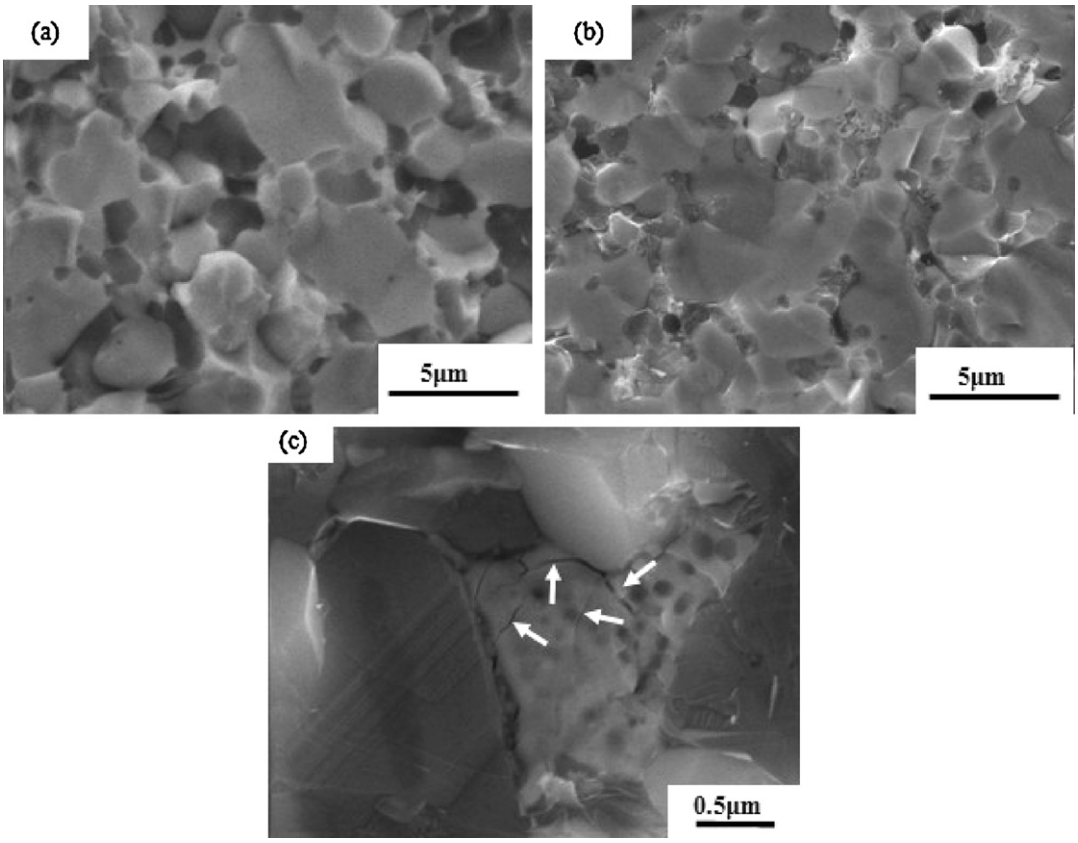

Fig. 4. SEM images of fracture surfaces of ZSY (a), and ZSY-1 (b and c) ceramics.

generation of large residual thermal stress in ZSY-1 ceramics. According to Selsing's model of a single spherical inclusion imbedded within an infinite isotropic elastic matrix, there would be thermal stress P presented on the spherical inclusion [15]:

$$P = \frac{\Delta\alpha\Delta T}{[(1+v_m)/2E_m + (1-2v_p)/E_p]}$$

where the subscripts m and p refer to the matrix and the particle, respectively, $\Delta\alpha = \alpha_p - \alpha_m$ is the thermal expansion mismatch, ΔT is the difference between the processing temperature and the room temperature, E is the elastic modulus, and v is the Poisson's ratio. In the ZSY-1 ceramics, the ZrB_2 was referred to as the matrix and the SiO_2 was referred to as inclusion. Based on Selsing's model, the estimated residual stress presented on SiO_2 was about -1.1 GPa. Therefore, the SiO_2-containing glassy phase pocket is under compressive stress in ZSY-1 ceramics. Due to the presence of SiO_2 particles, the residual thermal stress of ZSY-1 ceramics was larger than that of ZSY ceramics. Monteverde has reported that the freezing of thermal strained field in a particulate-reinforced ceramic–matrix composite had a beneficial effect on fracture toughness [16]. The large thermal residual stress in the ZSY-1 ceramics led to an increased fracture toughness, compared to the ZSY ceramics. So, applying the mechanical pressure already during the heating-up stage during SPS led to an increased fracture toughness of the ZrB_2–SiC–Yb_2O_3 ceramics. Careful observation reveals the presence of microcracks in the ZSY-1 ceramics, as indicated by the white arrows in Fig. 4(c). The microcracks could result from the mechanical testing process due to the brittle feature of the SiO_2-containing pocket.

4. Conclusion

The influence of the pressure loading cycle on ZrB_2–SiC–Yb_2O_3 ceramics was assessed. Microstructural observation revealed that nanometer-sized spherical SiO_2 particles are formed at the grain boundaries when already applying the load during the heating-up stage due to the entrapment of volatile species. The presence of SiO_2 particles led to a large thermal residual stress, and improved fracture toughness in the ZrB_2–SiC–Yb_2O_3 ceramics. Applying the load upon reaching the targeted SPS temperature allows evaporation of volatile species, avoiding the formation of SiO_2 precipitates and microcracks.

Acknowledgement

This work was financially supported by the research fund of K.U. Leuven in the framework of the Flanders-China bilateral project BIL 07/06, the Chinese Academy of Sciences under the Program for Recruiting Outstanding Overseas Chinese (Hundred Talents Program), the National Natural Science Foundation of China (no. 50632070), and the Science and Technology

Commission of Shanghai (no. 08520707800 and no. 09ZR1435500).

References

[1] W.G. Fahrenholtz, G.E. Hilmas, Refractory diborides of zirconium and hafnium, J. Am. Ceram. Soc. 90 (2007) 1347–1364.
[2] A.L. Chamberlain, W.G. Fahrenholtz, G.E. Hilmas, High-strength zirconium diboride-based ceramics, J. Am. Ceram. Soc. 87 (2004) 1170–1172.
[3] A. Bellosi, F. Monteverde, D. Sciti, Fast densification of ultra-high-temperature ceramics by spark plasma sintering, Int. J. Appl. Ceram. Technol. 3 (2006) 32–40.
[4] H.L. Wang, C.A. Wang, X.F. Yao, D.N. Fang, Processing and mechanical properties of zirconium diboride-based ceramics prepared by spark plasma sintering, J. Am. Ceram. Soc. 90 (2007) 1992–1997.
[5] D. Sciti, L. Silvestroni, M. Nygren, Spark plasma sintering of Zr- and Hf-borides with decreasing amounts of $MoSi_2$ as sintering aid, J. Eur. Ceram. Soc. 28 (2008) 1287–1296.
[6] S.Q. Guo, T. Nishimura, Y. Kagawa, J.M. Yang, Spark plasma sintering of zirconium diborides, J. Am. Ceram. Soc. 91 (2008) 2848–2855.
[7] I. Akin, M. Hotta, F.C. Sahin, O. Yucel, G. Goller, T. Goto, Microstructure and densification of ZrB_2–SiC composites prepared by spark plasma sintering, J. Eur. Ceram. Soc. 29 (2009) 2379–2385.
[8] Y. Zhao, L.J. Wang, G.J. Zhang, W. Jiang, L.D. Chen, Effect of holding time and pressure on properties of ZrB_2–SiC composite fabricated by the spark plasma sintering reactive synthesis method, Int. J. Refract. Met. Hard Mater. 27 (2009) 177–180.
[9] W.M. Guo, J. Vleugels, G.J. Zhang, P.L. Wang, O. Van der Biest, Effect of heating rate on densification, microstructure and strength of spark plasma sintered ZrB_2-based ceramics, Scripta Mater. 62 (2010) 802–805.
[10] W.M. Guo, Z.G. Yang, G.J. Zhang, Comparison of ZrB_2–SiC ceramics with Yb_2O_3 additive prepared by hot pressing and spark plasma sintering, Int. J. Refract. Met. Hard Mater. 29 (2011) 452–455.
[11] Z.X. Yuan, J. Vleugels, O. Van der Biest, Preparation of Y_2O_3-coated ZrO_2 powder by suspension drying, J. Mater. Sci. Lett. 19 (2000) 359–361.
[12] K. Vanmeensel, A. Laptev, J. Hennicke, J. Vleugels, O. Van der Biest, Modelling of the temperature distribution during field assisted sintering, Acta Mater. 53 (2005) 4379–4388.
[13] S.C. Zhang, G.E. Hilmas, W.G. Fahrenholtz, Pressureless sintering of ZrB_2–SiC ceramics, J. Am. Ceram. Soc. 91 (2008) 26–32.
[14] P.D. Miller, J.G. Lee, I.B. Cutler, The reduction of silica with carbon and silicon carbide, J. Am. Ceram. Soc. 62 (1979) 147–149.
[15] J. Selsing, Internal stresses in ceramics, J. Am. Ceram. Soc. 44 (1961), p. 419-419.
[16] F. Monteverde, Ultra-high temperature HfB_2–SiC ceramics consolidated by hot-pressing and spark plasma sintering, J. Alloys Compd. 428 (2007) 197–205.